Journal of Alloys and Compounds 513 (2012) 539–545

Contents lists available at SciVerse ScienceDirect

Journal of Alloys and Compounds

journal homepage: www.elsevier.com/locate/jallcom

First principle calculations of the electronic and optical properties of pure and (Mo, N) co-doped anatase TiO_2

Matiullah Khan, Junna Xu, Ning Chen, Wenbin Cao*

Department of Inorganic Nonmetallic Materials, School of Materials Science and Engineering, University of Science and Technology Beijing, Beijing 100083, China

ARTICLE INFO

Article history:
Received 26 August 2011
Received in revised form 31 October 2011
Accepted 1 November 2011
Available online 9 November 2011

Keywords:
Density functional theory
(Mo
N) co-doped TiO_2
Optical properties
Photocatalytic activity

ABSTRACT

Density functional theory calculations were performed in order to investigate the effect of (Mo, N) co-doping on the electronic and optical properties of anatase TiO_2. Comparative theoretical study is organized using different doping models including single Mo doping, single N doping in anatase TiO_2 and three different models of (Mo, N) co-doped TiO_2 regarding the position of the dopants with respect to each other. Mo doping in anatase TiO_2 reduced the band gap of pure TiO_2 from 2.12 eV to 1.90 eV by introducing Mo 4d state below the conduction band and shifted the Fermi level from the top of the valence band to the bottom of the conduction band which verifies the n-type doping nature of Mo in TiO_2. Isolated N 2p state was created above the top of the valence band due to the N doping and the band gap of N–TiO_2 was effectively reduced to about 0.78 eV; however the unoccupied N 2p states annihilate the electron–hole pairs which will limit the efficiency of N–TiO_2 in visible light photocatalytic activity. (Mo, N) co-doped TiO_2 has narrowed band gap of about 1.50 eV and simultaneous impurity states, one is above the top of the valence band (N 2p) and the other is just below the conduction band (Mo 4d). The introduction of Mo 4d state changes the character of N 2p states from unoccupied to occupied states which will lead to removal of the electron–hole recombination center and enhance the visible light photocatalytic activity. Furthermore, optical absorption coefficient spectra results show that (Mo, N) co-doping in anatase TiO_2 can have enhanced optical absorption in the visible region compared with that of N–TiO_2 and Mo–TiO_2, which is attributed to the reduced recombination centers. It is argued that (Mo, N) co-doped TiO_2 shows enhanced visible light photocatalytic activity due to the effective utilization of electron–hole pairs in the oxidation/reduction process.

1. Introduction

TiO_2 photocatalyst has attracted continuously increasing attention of researchers due to its wide range of potential applications in the quantitative destruction of undesirable chemical containments in water and air which gives a reasonable solution to the water and air pollution [1–3]. The excellent properties of TiO_2, such as non-toxicity, strong oxidation power, highest light-conversion efficiency, and high stability towards photocorrosion makes it more promising material for the photocatalytic processes [4–6]. However, its efficiency is limited in most of the applications because the generation of electrons–hole pairs (EHPs) in anatase TiO_2 is only possible when excited by ultraviolet (UV) due to the wide band gap. Enhanced utilization of the TiO_2 photocatalyst is possible by shifting its absorption edge towards visible light region which constitutes about 45% of the solar spectrum [7–9]. Among the various techniques, doping of foreign elements into TiO_2 is considered as one of the promising methods for shifting its absorption edge towards visible region [10]. Non-metal doping extends the photoresponse of TiO_2 from UV to visible light by introducing impurity states in the band gap or narrowing the effective band gap [11]. Since the pioneering work of Asahi et al. [12] the nitrogen (N) doping in TiO_2 is considered to be a prominent method for band gap narrowing of TiO_2, which is widely studied with the help of experimental [13–15] as well as theoretical tools [16,17]. However, the N doping will create the localized N 2p states just above the valence band acting as the trap for photogenerated carriers and decreases the photogenerated current which consequently limits the efficiency of N doped TiO_2 in the photocatalytic process [18,19]. Transition metals doping is also effective in generating visible light photocatalytic activity but its efficiency will be reduced due to the presence of the localized d states and the carrier recombination centers [20]. In order to solve these problems, the concept of metal-non-metal co-doping has been introduced which was found to be successful [21–24].

Molybdenum (Mo) is a transition metal and its doping in TiO_2 can effectively shift the absorption edge of TiO_2 towards visible light region. Due to the similarity in ionic size of Mo^{6+} (0.062 nm)

* Corresponding author. Tel.: +86 10 62332457; fax: +86 10 62332457.
E-mail address: wbcao@ustb.edu.cn (W. Cao).

0925-8388/$ – see front matter © 2011 Elsevier B.V. All rights reserved.
doi:10.1016/j.jallcom.2011.11.002

and Ti^{4+} (0.068 nm), Mo substitution at Ti sites causes minimum lattice distortion and results in stable doped model [25]. Jeon et al. [26] prepared Mo/Ti mixed oxide photocatalyst with varying Mo^{5+} content from 0 mol% to 2.5 mol% which showed shift in the absorption edge towards visible light. 2.5% Mo/Ti sample showed best visible light absorption and the band gap was effectively reduced about 0.22 eV compared with that of the pure TiO_2 [26]. N doping in TiO_2 lattice is effective in narrowing the band gap of TiO_2 because the N 2p states either introduce isolated states close to the valence band [27] or mix with O 2p states to reduce the band gap effectively [28]. (Mo, N) co-doping in TiO_2 will enhance the visible light absorption and the corresponding photocatalytic activity due to the decreased amount of the electron–hole pairs recombination centers.

In the present work we report the density functional theory calculation about electronic and optical properties of (Mo, N) co-doped anatase TiO_2 system. Mo at the Ti sites and N at the O sites were introduced in the TiO_2 supercell and then the system was geometrically optimized, after which its electronic and optical properties were evaluated. Enhanced band gap narrowing was found for the co-doped system because that the Mo doping would introduce defect states below the conduction band while the N doping would introduce impurity states above the valence band. It is argued that optimal concentrations of both the dopants would effectively shift the absorption edge towards visible light and enhance the visible light photocatalytic activity.

2. Calculations

The calculations were performed using spin polarized density functional theory (DFT) with the Perdew–Burke–Eruzerhof (PBE) [29] functional in the framework of generalized gradient approximation (GGA). The electron wave function was expanded in plane waves up to a cut-off energy of 380 eV with the fine set of Monkhorst–Pack *k*-points mesh [30]. CASTEP code [31] of material studio was used for all the theoretical calculation. The ions–electrons interaction was modeled by Vanderbilt-type ultrasoft pseudopotential [32]. The valence electrons configuration for the O, Ti, N, and Mo was $2s^2\ 2p^4$, $3s^2\ 3p^6\ 3d^2\ 4s^2$, $1S^2\ 2S^2\ 2P^6$ and $4s^2\ 4p^6\ 4d^5\ 5s^1$, respectively. In order to make stable configurations of the pure and doped models, all the structures were geometrically optimized using BFGS [33]. The models were converged by setting the value of displacement equal to 5×10^{-5} nm and the total energy difference become equal to 5×10^{-6} eV/atom [30].

The doped system consists of $2 \times 2 \times 1$ anatase TiO_2 supercell with 48 atoms in total. N doping in the anatase TiO_2 supercell was performed by replacing single O atom by N atom at its regular lattice site, and similarly Mo doped anatase TiO_2 was obtained when the Ti atom was replaced by Mo atom. For co-doping, O atom was replaced by N atom while Ti atom was replaced by Mo atom simultaneously. Three different models were constructed for the co-doping system in order to investigate the effect of the location of different dopants on the electronic and optical properties of the obtained models. In the first model, N and Mo were doped adjacently to one another by replacing the O and Ti atoms respectively, which was labeled as MoN-1. In the second model doped N and Mo were placed at a distance of 3.817 Å which is represented as MoN-2, while in the third model the distance between the doped N and Mo were increased to 7.227 Å and it is labeled as MoN-3 for simplicity. All the different doped models were geometrically optimized and then its electronic and optical properties were evaluated. The configurations of the different models are shown in Fig. 1.

Interactions of photons of suitable frequency with the orbital electrons shift the electron from the valence band to conduction band which can also be described as the transition between occupied and unoccupied states. These transitions will give spectra which can be described by the joint density of states between valence and conduction bands. The optical properties of materials can be measured from the complex dielectric function which consists of real part $\varepsilon_1(\omega)$ and imaginary part $\varepsilon_2(\omega)$, in which the real

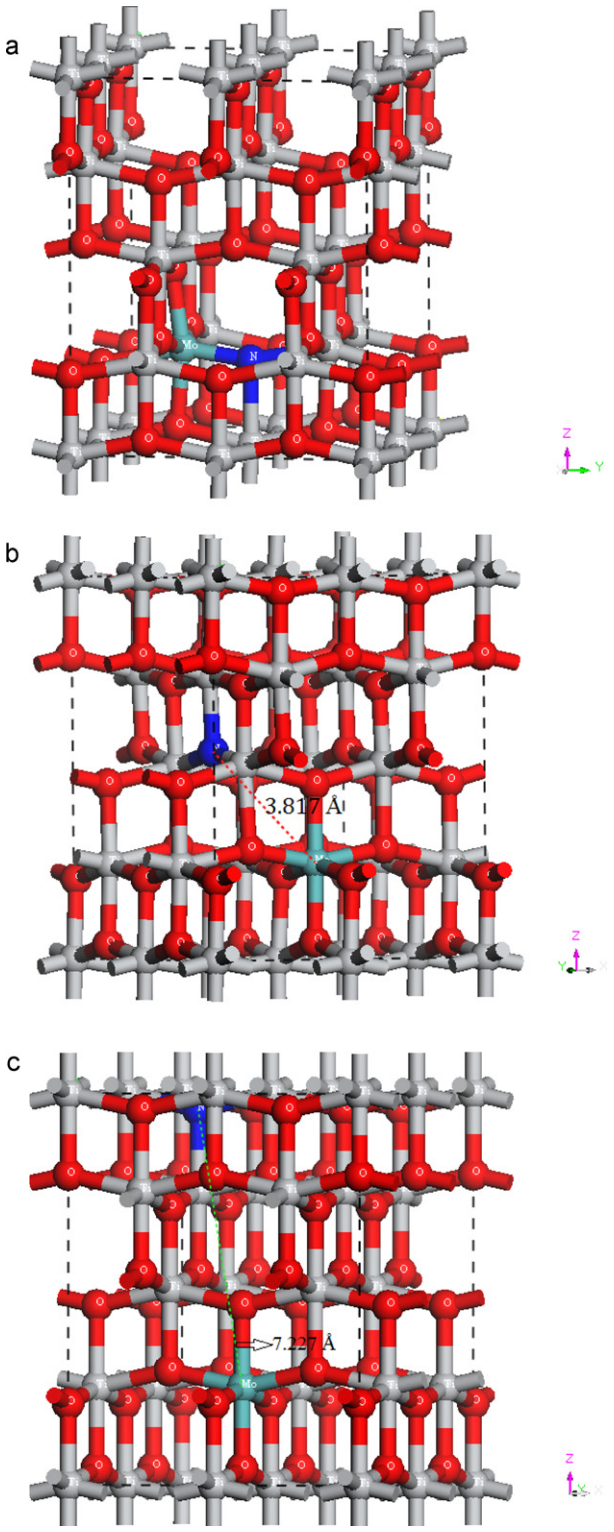

Fig. 1. Different doping models with respect to the location of substitutionaly doped N and Mo in the anatase TiO_2 supercell, (a) MoN-1, (b) MoN-2 and (c) MoN-3. The red, gray, blue, and cyan colors represent oxygen, Titanium, Nitrogen and Molybdenum atoms respectively. (For interpretation of the references to color in this figure legend, the reader is referred to the web version of the article.)

Table 1
Averaged bond lengths of the pure and different doped models after geometrical optimization.

Bond length (Å)	Pure TiO_2	Mo–TiO_2	N–TiO_2	MoN-1	MoN-2	MoN-3
Ti–O	1.9673	1.9483	1.9482	1.9458	1.9530	1.9527
O–O	2.7049	2.6906	2.6916	2.7082	2.7347	2.7339
N–O	–	–	2.6850	2.6905	2.7786	2.7820
Ti–Mo	–	–	–	2.9674	–	–
N–Mo	–	–	–	1.7438	–	–

part can be calculated using Kramer–Kronig relationship. The imaginary part is related with the electronic absorption of the material and can be obtained from the momentum matrix elements between occupied and unoccupied states wave functions using proper selection rules. The real and imaginary parts of the dielectric function are further used to calculate the optical constants, in which the absorption coefficient $\alpha(\omega)$ is given in Eq. (1) [32,34,35].

$$\alpha(\omega) = \sqrt{2}\omega\left[\sqrt{\varepsilon_1^2(\omega) + \varepsilon_2^2(\omega)} - \varepsilon_1(\omega)\right]^{1/2} \quad (1)$$

3. Results and discussion

3.1. Optimized structure properties

After geometrical optimization the obtained lattice parameters for pure TiO_2 are; $a = 3.806$ Å, and $c = 9.8654$ Å which are consistent with the results of Long et al. [36]. However, they were overestimated compared with those of the experimental data, $a = 3.782$ Å and $c = 9.502$ Å [37]. In order to check the lattice deformation, the average bond lengths of the doped TiO_2 after geometrical optimization were calculated and the results are listed in Table 1. In pure TiO_2, the averaged Ti–O bond and O–O bond length is 1.9673 Å and 2.7049 Å, which are slightly shortened after individual Mo and N doping. It is interesting to note that the averaged Ti–O and O–O bond lengths for N–TiO_2 and Mo–TiO_2 is nearly the same, but both of them have little change compared with those of pure TiO_2, which shows that the substitutional N doping at O sites and substitutional Mo doping at Ti sites will not cause large lattice distortion and therefore it is preferred. Among all the co-doped models, the MoN-1 models described a very little lattice deformation after (Mo, N) co-doping compared with those of the pure and individual Mo and N doped TiO_2. While the averaged Ti–O bond length of MoN-2 and MoN-3 are similar to that of the pure TiO_2; however large difference was found between the average O–O bond lengths. So, among all the individual Mo or N doped or co-doped models, the MoN-1 has very little lattice distortion and it is considered that this system will be more stable.

3.2. Electronic properties

The calculated band structures of the pure TiO_2 and different doped models are presented in Fig. 2. The band gap of the pure anatase TiO_2 is 2.12 eV, which is the same with that of the recently published theoretical calculation [38]. However, the calculated band gap was underestimated compared with that of the experimental data of 3.20 eV due to the well-known drawback in DFT calculations [39]. The GGA method is not able to describe the states correctly at the case when close to the conduction band of the semiconductors which leads to the underestimated results [40]. The GGA + U calculation was introduced to obtain closer values to the experimental band gaps [41]. In the structure of Mo-TiO_2 (Fig. 2b), one Mo atom was substitutionaly doped at the Ti site which shifts the Fermi level from the top of the valence band to the bottom of the conduction band. This shifting of the Fermi level shows the n-type doping nature of Mo in TiO_2 [42] and the band gap is effectively narrowed by introducing impurity states below the conduction band due to the Mo doping. In this case, the band gap was reduced from 2.12 eV (pure TiO_2) to 1.90 eV (Mo–TiO_2) and the reduction was about 0.22 eV. N substitution at the O site introduced N 2p states located at above the valence band maximum of TiO_2 which reduced the calculated band gap of TiO_2 from 2.12 eV to 1.34 eV. That is, N doping effectively narrowed the band gap of anatase TiO_2 to a value of about 0.78 eV by introducing the impurity states which were located at 0.63 eV above the valence band maximum. Literature shows that the visible light absorption in N–TiO_2 is still debatable. Asahi et al. [12] reported that substitutionaly doped nitrogen atom at the oxygen sites reduce the band gap of TiO_2 by mixing N 2p states with O 2p states and make it capable to absorb visible light. Some authors [43] argued that band gap of TiO_2 was narrowed because N doping introduces isolated N 2p state above the O 2p state which makes the TiO_2 visible light responsive. Theoretical calculation of Di Valentin et al. [44,45] showed that substitutional N doping in TiO_2 creates N 2p states localized at about 0.14 eV above the valence band maximum, while the interstitial N doping leads to the creation of occupied N 2p localized states located at about 0.73 eV above the top of the valence band of TiO_2 which are responsible for the visible light response in the N doped TiO_2. Substitutional N doping creates partially occupied N 2p states in the band gap of TiO_2 because of the deficiency of electron on N 2p level due to the reduction of Ti^{4+} to Ti^{3+} occurs in N–TiO_2 as a result of charge imbalance between O^{2-} ions and N^{3-} ions [46]. In our case, the N 2p states are located at about 0.63 eV above the valence band maximum (VBM) which makes the TiO_2 capable to absorb light in the visible region. However, in the case of visible light photocatalytic activity this partially occupied impurity states will act as a trap for the excited electrons, which promote electrons–hole pairs recombination and limit the efficiency of N–TiO_2 in the visible light region [3,30,36]. In order to solve the problem of carrier recombination and to enhance of visible light photocatalytic activity, Ti atom in the supercell was replaced by Mo atom and then a partially occupied impurity band was introduced below the conduction band minimum which is mainly composed of d_{xy} components. This impurity states will then extend the absorption edge of the pure TiO_2 towards visible light region.

(Mo, N) co-doped TiO_2 will enhance the visible light photocatalytic activity because of introducing impurity states above the VBM as well as below the conduction band minimum simultaneously. It is argued that this co-doping will modify the valence and conduction band because N has different atomic p orbital energy compared with that of O, while Mo also has different atomic d orbital energy relative to that of Ti. As to the co-doped system, we introduced three different models regarding the position of the dopants with respect to each other. The Mo and N were doped in the TiO_2 lattice substitutionaly at the adjacent positions with distance of 3.817 Å, and little far from one another having distance of 7.227 Å which were represented by MoN-1, MoN-2, and MoN-3, respectively. The electronic structures and optical properties of the MoN-2 and MoN-3 model were nearly the same. However MoN-1 presented reduced band gap of 1.50 eV and best optical absorption among all of them. It is concluded that adjacent location (MoN-1) of the dopants will be the best as this model gives

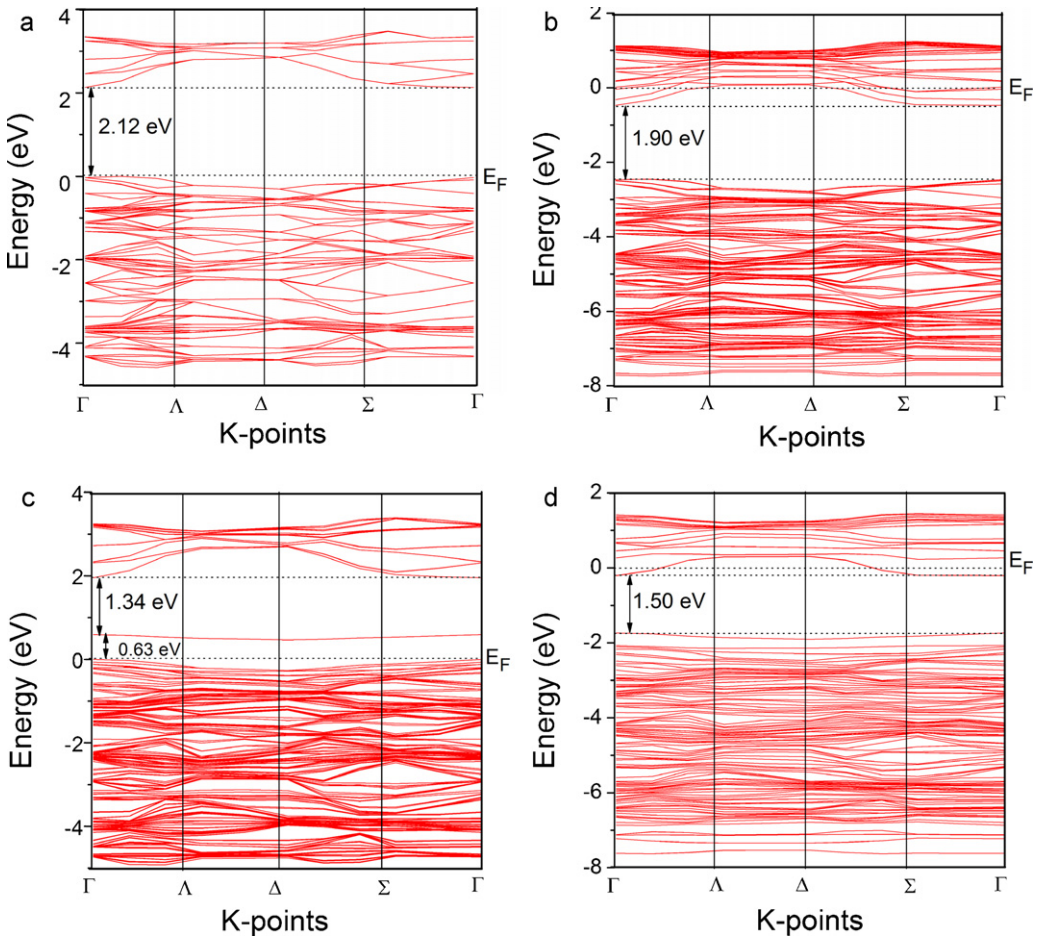

Fig. 2. Band gap structure of (a) Pure TiO_2, (b) Mo–TiO_2, (c) N–TiO_2, and (d) (Mo, N) co-doped TiO_2. The E_F represents the Fermi level.

minimum lattice distortion (Table 1) compared with that of the other models along with enhanced electronic and optical properties.

To further explore the modifications in the band structure and the origin of visible light absorption, the density of states (DOS) of different doped models have been calculated as indicated in Fig. 3. Partial Density of States (PDOS) of the pure TiO_2 (Fig. 3a) shows that the valence band edge of TiO_2 mainly consists of O 2p states while the conduction band is predominantly composed of Ti 3d states. This describes the intrinsic band gap nature of the pure TiO_2 which can be changed by doping different elements; just like in this case we doped Mo and N substitutionaly at the Ti and O sites respectively. When the substitutional N is introduced at the O sites, it acts as a single acceptor due to N having one electron less than O which leads to the creation of acceptor N 2p states located at above the valence band maximum of TiO_2. This N 2p states are responsible for the band gap narrowing and consequently its visible light absorption; however these states may act as recombination ones as aforementioned, which annihilate photogenerated electron-hole pairs. Mo doping in TiO_2 introduces shallow donor states which are located below the conduction band minimum and extends the absorption edge of TiO_2 towards visible light. Fig. 3c shows that the Mo 4d states is located just below the conduction minimum which effectively reduces the band gap of TiO_2 from 2.12 eV to 1.90 eV. Shifting of the Fermi level from the top of the valence band to the bottom of the conduction band is found after Mo doping in TiO_2 which shows that Mo is a suitable n-type dopant. PDOS of the co-doped model (Fig. 3d) shows that simultaneously N 2p states are introduced above the VBM while Mo 4d states are introduced below the conduction band minimum. The band gap of TiO_2 is effectively modified because N has different atomic p orbital energy compared with that of O, while Mo has also different atomic d orbital with respect to that of Ti. It is observed that the N 2p state is below the Fermi level after co-doping, which indicates that N 2p states are occupied and cannot act as traps for electron–hole pairs and will consequently increases the visible light photocatalytic activity of the co-doped model. It is evident that the incorporation of Mo into the N doped TiO_2 changes the character of N 2p states from unoccupied to occupied states, which will effectively enhance the optical properties and visible light photocatalytic activities. It is argued that [36] for the highest occupied molecular orbital, the electron transfer from the fully occupied states to the conduction band minimum will reduce the photon transition energy significantly and thus decrease the electron–hole pairs recombination. Fig. 3d indicates that the valence band of the co-doped TiO_2 is predominantly made of O 2p states and the N 2p states located at the above of the valence band maximum while the conduction band is composed of Ti 3d and Mo 4d orbitals. Fig. 3e shows the total density of states (TDOS) of the pure TiO_2 as well as of the different doped models. Compared with that of pure TiO_2, the conduction band of the N–TiO_2 remains unchanged; however the valence band maximum is distorted slightly due to the introduction of N 2p states just above the valence band maximum. Mo doping changed the location of the Fermi level from the top of the valence band to the bottom of the conduction band and narrowed the band gap due to the creation of impurity states below the conduction band. Among all the doped models, the (Mo, N) co-doped TiO_2 (MoN-1) provided narrowed band gap due to the

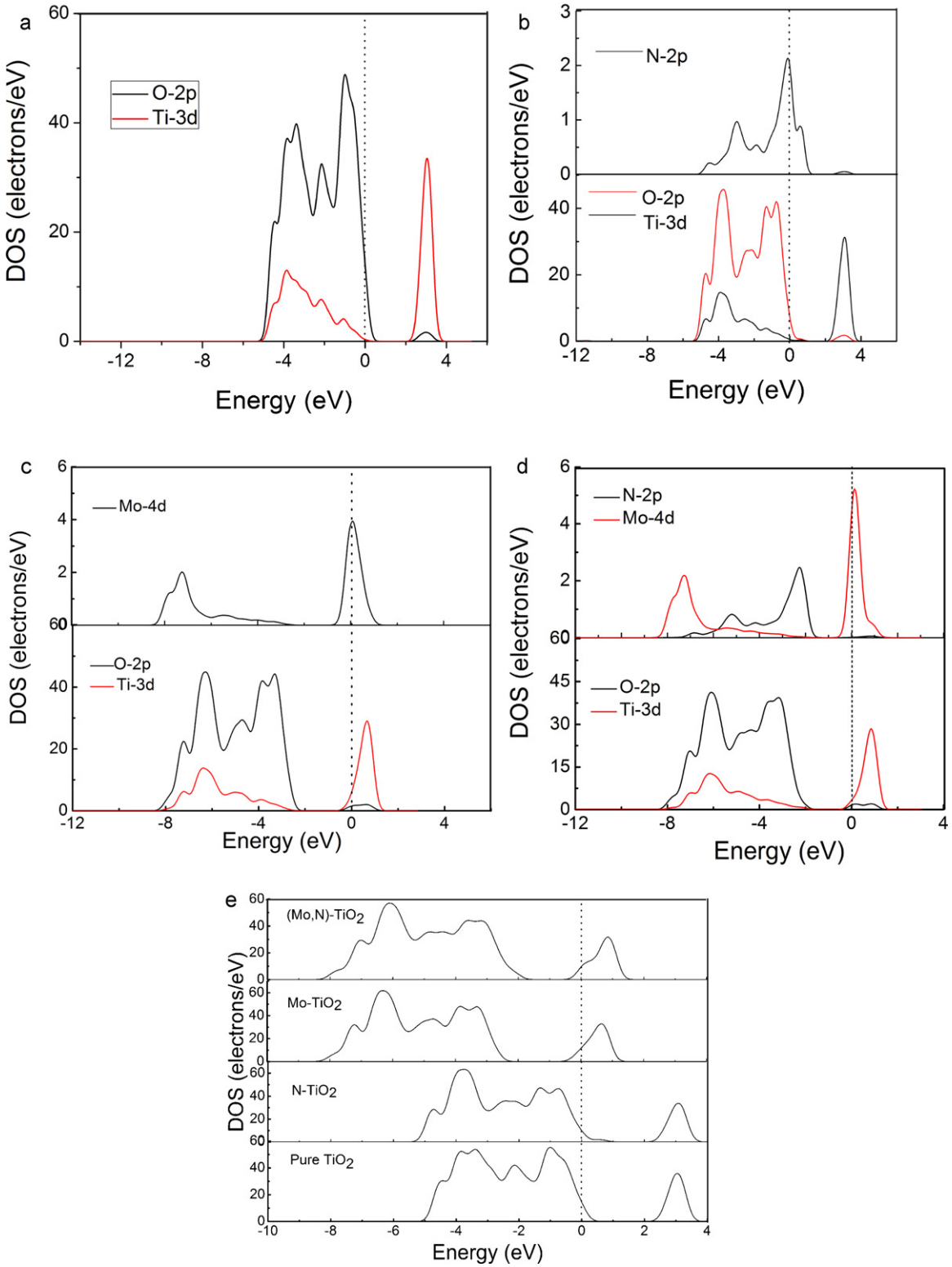

Fig. 3. PDOS of the (a) Pure TiO_2, (b) N-TiO_2, (c) Mo–TiO_2, and (d) (Mo, N) codoped TiO_2 (MoN-3). The comparisons of the TDOS of the pure and different doped models are depicted in (e). The vertical dotted line at $E = 0$ eV, represent the Fermi level.

simultaneous states introduced by Mo and N below the conduction band and at the top of the valence band respectively. All the doped models have narrowed band gap compared with that of the pure TiO_2 and the related TDOS were also consistent with the band structures.

3.3. Optical properties

The optical absorption spectra of the pure and different doped models were calculated using the obtained electronic structures and presented in Fig. 4. As the calculated band gap of anatase TiO_2

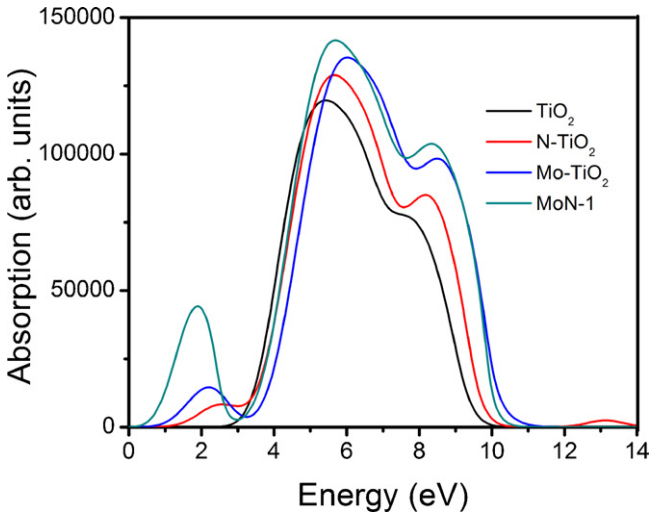

Fig. 4. The comparison of the optical absorption of pure and different doped models is described.

is 2.12 eV which is less than that of the experimental data of 3.2 eV, therefore a scissor approximation [29] of 1.08 eV is applied for calculating the optical properties of the pure and doped models in order to fit it to the experimental result. It is clarified that pure TiO_2 has no absorption in visible light range and responds only to UV light. Our calculations show that the optical absorption edge for the pure TiO_2 is 3.2 eV as indicated in Fig. 4, which is exactly the same to the experimental value of the band gap of anatase TiO_2 and consistent with other theoretical calculations [38]. These optical excitations correspond to the pure band gap of anatase TiO_2 and will arise from the shifting of electrons from the O 2p to Ti 3d states. Absorption spectra show that doping foreign atoms in the TiO_2 lattice has shifted the absorption edge towards visible light range; however the shifting of absorption edge depends upon the nature of the atom doped. The shifting of absorption edge is more pronounced in the (Mo, N) co-doped TiO_2 (MoN-1) compared with that of the individual Mo or N doped TiO_2. For all the doped and undoped models, the main absorption locates in the UV light region due to the intrinsic band gap of anatase TiO_2; however for the doped models, the ranges of visible light absorption have also been found differs for different doped models. The absorption edge is shifted to 1.5 eV for N–TiO_2 which is consistent with the recent theoretical calculations [35]. This narrowed band gap of N–TiO_2 will effectively absorb light in visible range as a result of transitions of electrons from O 2p to Ti 3d states through the N 2p state due to the N doping. The electrons will be firstly shifted from O 2p states to N 2p state and will be further transferred to the conduction band (Ti 3d).

Optical absorption spectrum of Mo–TiO_2 shows absorption edge at 1.2 eV which effectively absorbs light in the visible region. These excitations may be corresponding to the shifting of electrons from O 2p to Mo 4d states which is consistent with recent theoretical calculations [42]. It is argued [42] that the light absorption in the low energy region in Mo–TiO_2 may be attributed to intra-band transition of the Mo 4d and Ti 3d states. Enhanced visible light absorption as well as the UV light absorption has been found for (Mo, N) co-doped TiO_2 (MoN-1) compared with that of N–TiO_2 and Mo–TiO_2 which is attributed to narrowed band gap due to the co-doping effect. The absorption edge for (Mo, N) co-doped TiO_2 is located at 0.6 eV and its absorption peak is at 1.9 eV which shows that the co-doping effectively shifted the absorption edge and enhanced the visible as well as the UV light absorption. The visible light absorption in the co-doped models maybe correspond to transitions of electrons from O 2p to Mo 4d through N 2p states and then to the Ti 3d states. Some absorption in the low energy region maybe come from the intra-band transitions between O 2p to N 2p, N 2p to Mo 4d, and Mo 4d to Ti 3d states. From the optical absorption spectra of the pure and doped models, the enhanced visible light absorption of (Mo, N) co-doped TiO_2 is attributed to the creation of impurity states in the band gap due to the N and Mo doping. Regarding the different location of Mo and N with respect to one another in the TiO_2 lattice, MoN-1 has the best optical absorption in the visible light region. That is, MoN-1 has the enhanced visible light photocatalytic activity and it is a good potential candidate for photoelectrochemical applications.

4. Conclusions

In the current research work, the electronic and optical properties of the pure anatase TiO_2, Mo–TiO_2, N–TiO_2, and (Mo, N) co-doped anatase TiO_2 have been calculated and analyzed using first principle calculations. N doping will effectively reduce the band gap of anatase TiO_2; however the unoccupied N 2p states above the valence band will act as an electron–hole pair recombination center, which will limit the efficiency of N–TiO_2 in visible light photocatalytic activity. Mo doping in N–TiO_2 changes the nature of N 2p states from unoccupied to occupied states, which will lead to the absence of electron–hole pair recombination centers and increase visible light photocatalytic activity. Bond length calculation results show that among three different (Mo, N) co-doping models, the MoN-1 model having adjacent location of the dopants provides minimum lattice deformation compared with that of the pure TiO_2 which is considered as the most favorable one. Enhanced visible light absorption is obtained for MoN-1 model compared with that of N–TiO_2, Mo–TiO_2, and other co-doping models. That is, model MoN-1 will provide enhanced visible light photocatalytic activity due to the reduced electron–hole pair recombination centers and the stable structure.

Acknowledgements

This work has been financially supported by National Natural Science Foundation of China under the grant number of 51072019 and the Opening Project of State Key Laboratory of High Performance Ceramics and Superfine Microstructure under the grant SKL201112SIC. It is gratefully acknowledged.

References

[1] Y. Liao, W. Que, J. Alloys Compd. 505 (2010) 243.
[2] Y. Liu, F. Xin, F. Wang, S. Luo, X. Yin, J. Alloys Compd. 498 (2010) 179.
[3] X. Ma, L. Miao, S. Bie, J. Jiang, Solid State Commun. 150 (2010) 689.
[4] S. Li, Q. Shen, J. Zong, H. Yang, J. Alloys Compd. 508 (2010) 99.
[5] F. Spadavecchia, G. Cappelletti, S. Ardizzone, M. Ceotto, L. Falciola, J. Phys. Chem. C 115 (2011) 6381.
[6] H. Liu, Y. Wu, J. Zhang, ACS Appl. Mater. Interfaces 3 (2011) 1757.
[7] X. Liu, Z. Liu, J. Zheng, X. Yan, D. Li, S. Chen, W. Chu, J. Alloys Compd. 509 (2011) 9970.
[8] R.M. Mohamed, E.S. Aazam, J. Alloys Compd. 509 (2011) 10132.
[9] U.O.A. Arıer, F.Z. Tepehan, J. Alloys Compd. 509 (2011) 8262.
[10] H. Pan, Y.W. Zhang, V.B. Shenoy, H. Gao, J. Phys. Chem. C 115 (2011) 12224.
[11] D. Wu, M. Long, W. Cai, C. Chen, Y. Wu, J. Alloys Compd. 502 (2010) 289.
[12] R. Asahi, T. Morikawa, T. Ohwaki, K. Aoki, Y. Taga, Science 293 (2001) 269.
[13] S. Livraghi, M.R. Chierotti, E. Giamello, G. Magnacca, M.C. Paganini, G. Cappelletti, C.L. Bianchi, J. Phys. Chem. C 112 (2008) 17244.
[14] H. Sun, Y. Bai, W. Jin, N. Xu, Sol. Energy Mater. Sol. Cells 92 (2008) 76.
[15] S. Hu, A. Wang, X. Li, H. Lowe, J. Phys. Chem. Solids 71 (2010) 156.
[16] Y. Yin, W. Zhang, S. Chen, S. Yu, Mater. Chem. Phys. 113 (2009) 982.
[17] L. Mi, Y. Zhang, P.N. Wang, Chem. Phys. Lett. 458 (2008) 341.
[18] X. Chen, C. Burda, J. Am. Chem. Soc. 130 (2008) 5018.
[19] A. Kubacka, G. Colon, M. Fernandez-Garcia, Catal. Today 143 (2009) 286.
[20] V. Stengl, S. Bakardjieva, J. Phys. Chem. C 114 (2010) 19308.
[21] M.E. Kurtoglu, T. Longenbach, K. Sohlberg, Y. Gogotsi, J. Phys. Chem. C 115 (2011) 17392.
[22] W. Zhu, X. Qiu, V. Iancu, X.Q. Chen, H. Pan, W. Wang, N.M. Dimitrijevic, T. Rajh, H.M. Meyer III, M.P. Paranthaman, G.M. Stocks, H.H. Weitering, B. Gu, G. Eres, Z. Zhang, Phys. Rev. Lett. 103 (2009) 226401.

[23] C.C. Pan, J.C.S. Wu, Mater. Chem. Phys. 100 (2006) 102.
[24] R. Long, N.J. English, Chem. Mater. 22 (2010) 1616.
[25] L.G. Devi, B.N. Murthy, S.G. Kumar, J. Mol. Catal. A: Chem. 308 (2009) 174.
[26] M.S. Jeon, W.S. Yoon, H. Joo, T.K. Lee, H. Lee, Appl. Surf. Sci. 165 (2000) 209.
[27] K. Yang, Y. Dai, B. Huang, S. Han, J. Phys. Chem. B 110 (2006) 24011.
[28] S. Yin, H. Yamaki, Q. Zhang, M. Komatsu, J. Wang, Q. Tang, F. Saito, T. Sato, Solid State Ionics 172 (2004) 205.
[29] M.G. Brik, I. Sildos, V. Kiisk, Phys. B 405 (2010) 2450.
[30] W. Shi, Q. Chen, Y. Xu, D. Wu, C. Huo, Appl. Surf. Sci. 257 (2011) 3000.
[31] S.J. Clerk, M.D. Segall, C.J. Pickard, P.J. Hasnip, M.I.J. Probert, K. Refson, M.C. Payne, Z. Kristallogr. 220 (2005) 567.
[32] J. Sun, H.T. Wang, J. He, Y. Tian, Phys. Rev. B 71 (2005) 125132.
[33] B.G. Pfrommer, M. Cote, S.G. Louie, M.L. Cohen, B. Pfrommer, J. Comput. Phys. 131 (1997) 233.
[34] S.M. Baizaee, N. Mousavi, Phys. B 404 (2009) 2111.
[35] L. Jia, C. Wu, S. Han, N. Yao, Y. Li, Z. Li, B. Chi, J. Pu, L. Jian, J. Alloys Compd. 509 (2011) 6067.
[36] R. Long, N.J. English, Chem. Phys. Lett. 478 (2009) 175.
[37] J.K. Burdett, T. Hughbanks, G.J. Miller, J.W. Richardson, J.V. Smith, J. Am. Chem. Soc. 109 (1987) 3639.
[38] Z. Zhou, M. Li, L. Guo, J. Phys. Chem. Solids 71 (2010) 1707.
[39] K. Yang, Y. Dai, B. Huang, Chem. Phys. Lett. 456 (2008) 71.
[40] X. Yu, C. Li, H. Tang, Y. Ling, T. Tang, Q. Wu, J. Kong, Comput. Mater. Sci. 49 (2010) 430.
[41] A.M. Czoska, S. Livraghi, M. Chiesa, E. Giamello, S. Agnoli, G. Granozzi, E. Finazzi, C. Di Valentin, G. Pacchioni, J. Phys. Chem. C 112 (2008) 8951.
[42] X. Yu, C. Li, Y. Ling, T. Tang, Q. Wu, J. Kong, J. Alloys Compd. 507 (2010) 33.
[43] H. Irie, Y. Watanabe, K. Hashimoto, J. Phys. Chem. B 107 (2003) 5483.
[44] C.D. Valentin, G. Pacchioni, A. Selloni, S. Livraghi, E. Giamello, J. Phys. Chem. B 109 (2005) 11414.
[45] C.D. Valentin, E. Finazzi, G. Pacchioni, A. Selloni, S. Livraghi, M.C. Paganini, E. Giamello, Chem. Phys. 339 (2007) 44.
[46] Y. Nakano, T. Morikawa, T. Ohwaki, Appl. Phys. Lett. 86 (2005) 132104.